Carbohydrate Polymers 101 (2014) 642–649

Contents lists available at ScienceDirect

Carbohydrate Polymers

journal homepage: www.elsevier.com/locate/carbpol

Melt-processed poly(vinyl alcohol) composites filled with microcrystalline cellulose from waste cotton fabrics

Xunwen Sun, Canhui Lu, Yong Liu, Wei Zhang, Xinxing Zhang*

State Key Laboratory of Polymer Materials Engineering, Polymer Research Institute of Sichuan University, Chengdu 610065, China

ARTICLE INFO

Article history:
Received 6 July 2013
Received in revised form 7 September 2013
Accepted 24 September 2013
Available online 3 October 2013

Keywords:
Waste cotton fabrics
Microcrystalline cellulose
Poly(vinyl alcohol)
Composites
Melt-processing

ABSTRACT

Waste cotton fabrics (WCFs), which are generated in a large volume from the textile industry, have caused serious disposal problem. Recycling WCFs into value-added products is one of the vital measures for both environmental and economic benefits. In this study, microcrystalline cellulose (MCC) was prepared by acid hydrolysis of WCFs, and used as reinforcement for melt-processed poly(vinyl alcohol) (PVA) with water and formamide as plasticizer. The microstructure and mechanical properties of the melt-processed PVA/MCC composites were characterized by Fourier transform infrared spectra, Raman spectra, differential scanning calorimetry, thermal gravimetric analysis, X-ray diffraction, tensile tests and dynamic mechanical analysis. The results indicated that MCC could establish strong interfacial interaction with PVA through hydrogen bonding. As a result, the crystallization of PVA was confined and its melting temperature was decreased, which was beneficial for the melt-processing of PVA. Compared with the unfilled PVA, the PVA/MCC composites exhibited remarkable improvement in modulus and tensile strength.

1. Introduction

It was reported that the annual production of cotton fabrics for textiles and other applications exceeded 28 million tons in 2009, which for about 2/5 of the global market of textile fibers (Engelhardt, 2010). Generally, used clothes and leftover materials of textile industry end in waste stations are usually landfilled or incinerated (Miranda, Sosa-Blanco, Bustos-Martinez, & Vasile, 2007). These disposing methods not only create environmental pollution but also lead to great waste of the valuable resources. Therefore, recycling waste cotton fabrics (WCFs) into value-added products is an attractive and viable option for both environmental and economic benefits.During recent years, a number of methods have been pursued for recycling WCFs to value-added products, such as preparing cellulose derivatives (Ratanakamnuan, Atong, & Aht-Ong, 2012; Xiong, Lu, Zhang, Zhou, & Zhang, 2013) and energy production (Isci & Demirer, 2007; Jeihanipour & Taherzadeh, 2009; Shen et al., 2013). One potential way to high-value utilizing WCFs is extracting microcrystalline cellulose (MCC) from WCFs (Chuayjuljit, Su-Uthai, Tunwattanaseree, & Charuchinda, 2009) and used as reinforcement for composite materials (Chuayjuljit et al., 2009; Chuayjuljit, Su-Uthai, & Charuchinda, 2012; Saowaroj, Su-Uthai, & Charuchinda, 2010; Spoljaric, Genovese, & Shanks, 2009) due to its unique chemical and physical properties (Haafiz, Eichhorn, Hassan, & Jawaid, 2013; Mathew, Oksman, & Sain, 2005). However, the combination of MCC with the matrix encounters a considerable problem associated with the incompatibility between the polar and hydrophilic MCC fiber and the non-polar and hydrophobic polymer matrix.

Recently, as a polar and biodegradable polymer, poly(vinyl alcohol) (PVA), which could be manufactured from non-petroleum resources has attracted world concerns for developing ecofriendly composites (Jia et al., 2007). PVA has a large number of hydroxyl groups along its polymer chains, and most of the hydroxyl groups could form either inter- or intra-molecular hydrogen bonds. Therefore, PVA is well suited for preparing composites with cellulose fiber because both of them are highly polar materials and the large amount of hydroxyl groups on these two materials may facilitate interfacial interactions through hydrogen bonding, leading to desirable adhesion at the PVA/cellulose fiber composites interfaces. However, to our best knowledge, most PVA/cellulose composites are limited in the solution processing (Cheng, Wang, & Rials, 2009; Ibrahim et al., 2010; Kadokawa, Takegawa, Mine, & Prasad, 2011; Nishio & Manley, 1998; Zia et al., 2012; Zuber et al., 2012), which could only yield low dimension PVA products because of the large consumption of energy and time at the dissolving and drying process. Thus, its application areas are significantly constrained. The melt-processing of PVA is a big challenge worldwide because its melting temperature (T_m) is very close to its decomposition temperature (T_d). Realization of melt-processing of PVA would be a great development in PVA industry. The author's laboratory (Zhen, Lu, Li, & Liang, 2012) has realized the melt-processing of PVA by using formamide and water as plasticizer which can form inter-molecular complexes with PVA through hydrogen bond.

* Corresponding author. Tel.: +86 28 85460607; fax: +86 28 85402465.
E-mail address: xxzwwh@scu.edu.cn (X. Zhang).

0144-8617/$ – see front matter © 2013 Elsevier Ltd. All rights reserved.
http://dx.doi.org/10.1016/j.carbpol.2013.09.088

This plasticization technology adopted for melt-processing of PVA is much more effective, simple and cost-saving compared with the traditional solution-based processing technology. The formamide/water compound plasticizer was also used in this work.

To our best knowledge, few publications have been reported concerning on PVA/MCC composites. The aim of this work was to prepare melt-processed PVA composites with formamide and water as plasticizers, using MCC which was extracted from the WCFs as reinforcement. The influence of MCC on the structure and properties of the PVA/MCC composites was investigated and discussed in detail.

2. Methods

2.1. Materials

Waste cotton fabrics (WCFs) were collected from tailoring workshops and subjected to cutting and shredding processes. Poly(vinyl alcohol) 1799, with degree of polymerization 1750 ± 50 and degree of alcoholysis of 99%, was provided by SINOPEC Sichuan Vinylon Works, China. Analytical grade formamide, sodium hydroxide, acetone, ethanol, hydrochloric acid, nitric acid and sulfuric acid were purchased from Chengdu Kelong Chemical Plant.

2.2. Preparation of MCC

MCC was prepared by hydrolyzing WCFs, and the procedure is according to Xiong, Zhang, Tian, Zhou, and Lu (2012) as follows: WCFs (100 g) and 700 mL of 3% NaOH were mixed and boiled with slow stirring for 6 h. After cooling, WCFs were washed by distilled water, followed by boiling with 0.6% NaClO for 30 min. Then they were washed by distilled water again. 68% Nitric acid, 37% hydrochloric acid and distilled water were mixed at a ratio of 1:2:2 (v/v) to obtain the mixed acid. The acid mixture (700 mL) was used to hydrolyze WCFs at 60 °C for 1 h to produce MCC. The obtained MCC was filtered and washed to reach neutrality by distilled water. Further wash by 95% ethanol was done until the filtrate was colorless. Finally it was washed by acetone and filtrated using a vacuum pump. It was dried at 80 °C and smashed to obtain product. It was found the yield of MCC obtained from WCFs is as high as approximately 90%, which is higher than wood, agricultural residues and other materials (El-Sakhawy & Hassan, 2007). WCFs appear a good raw material to prepare MCC, since it presents high cellulose content (Miranda et al., 2007).

2.3. Preparation of PVA/MCC composites through melt-processing

PVA, water, formamide (2:1:1 in weight) and MCC were mixed in a high-speed mixer (1000 rpm) at room temperature for 10 min. After that, these mixtures were sealed for a week to achieve sufficient diffusion of plasticizers into PVA. The content of additional MCC was expressed as parts per hundreds of PVA (0, 5, 10, 15, 20 phr), respectively. The PVA blends were melt-mixed using a Brabender Plasti-corder PL2000 mixing machine with a mixing volume of 50 cm^3 at 150 °C and 30 rpm for 10 min. After the blends were taken out of the mixing chamber, they were cooled to room temperature and broken up with a crusher. These mixtures were molded using a mini-injection molding machine (HAAKE Minijet, USA) into samples with the dimension of 75 mm × 4 mm × 2 mm (length × width × thickness). The barrel temperature of the Minijet was 170 °C and the mold temperature was 80 °C. The injection pressure and the holding pressure were 60 MPa and the holding time was 10 s.

2.4. Characterization

2.4.1. FTIR analysis

Fourier transform infrared spectra (FTIR) of the PVA/MCC composites were conducted by means of a Nicolet 560 spectrophotometer (USA), taking over 20 scans for each sample with a resolution of 2 cm^{-1}, ranging from 400 to 4000 cm^{-1}. The samples were prepared by using the KBr-disk method. All the samples were dried in vacuum oven at 60 °C for 24 h before testing.

2.4.2. FT-Raman

Raman spectra were recorded on a Bruker FT-Raman spectrometer VERTEX-70 (Bruker Optics, Germany) using a diode pumped Nd:YAG laser at an operating wavelength of 1064 nm. The measurements were performed using the 180° angle scattering geometry with 100 scans and a laser power of 500 mW at the sample location. Samples of PVA/MCC composites were from the injection molding. The interferograms were apodized with the Blackman–Harris 4-term function and Fourier-transformed to obtain spectra with a resolution of 4 cm^{-1}.

2.4.3. Thermal property analysis

Curves of differential scanning calorimetry (DSC) analysis for the samples were recorded on a NETZSH 204 DSC differential scanning calorimeter under a flowing N_2 with sample weight 5 mg. The thermal properties of all samples were measured by heating from ambient temperature to 250 °C at a heating rate of 10 °C/min. The degree of crystallinity of PVA was calculated based on the following equation.

$$\chi_c = \frac{\Delta H_m}{w\Delta H_m^0} \quad (1)$$

where w is the weight fraction of PVA matrix in the composites, ΔH_m is the heat of fusion and ΔH_m^0 is the heat of fusion of 100% crystalline PVA which has a value of 161 J/g (Uddin, Fujie, Sembo, & Gotoh, 2012).

Thermogravimetric analysis (TGA) under nitrogen purge (flow rate about 100 mL/min) was performed using a TA-2000 analyzer (TA Instrument), the scanning rate of 10 °C/min and temperature range of 40–600 °C was used. Samples of about 5 mg were placed in an open alumina crucible. All the samples were vacuum oven dried at 60 °C for 24 h before testing.

2.4.4. XRD

X-ray diffraction (XRD) patterns were collected on a Philips Analytical X'Pert X-diffractometer (Philips Co., Netherlands), using Cu-Ka radiation (λ = 0.1540 nm) at an accelerating voltage of 40 kV and the current of 40 mA. The data were collected from 2θ = 5–60° with a step interval of 0.03°.

The crystallite size was calculated by using the Scherrer equation:

$$D = \frac{K\lambda}{\beta_{1/2}\cos\theta} \quad (2)$$

where D is the "apparent crystallite size", and $\beta_{1/2}$ is the full width of the diffraction peak measured at half maximum height (FWHM), constant K equals to 0.94.

2.4.5. SEM studies

The morphology of the MCC particles and the cryofractured surface of PVA/MCC composites were investigated by scanning electron microscope (SEM, JEOL JSM-5600, Japan) with an accelerating voltage of 20 kV. The samples were mounted on metal stubs using double side adhesive tapes. The samples were previously sputter coated with gold to prevent charging on the surface.

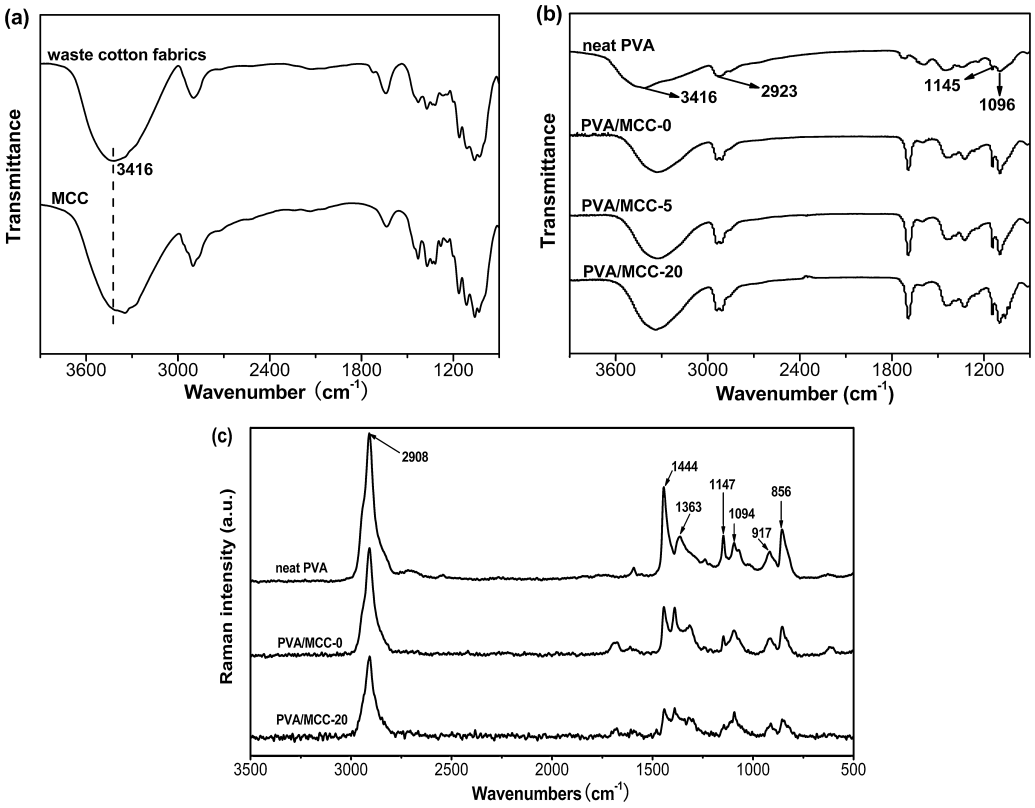

Fig. 1. (a) FTIR spectra of WCFs and MCC, (b) FTIR spectra of neat PVA and PVA/MCC composites, and (c) FT-Raman spectra of neat PVA and PVA/MCC composites.

2.4.6. Molau test

The Molau test (Molau & Wittbrodt, 1968) was used to study the interfacial interaction between the PVA matrix and MCC. In a typical example, melt-processed PVA/MCC composite (20 phr MCC content) and PVA/MCC composite film prepared by solution casting method (20 phr MCC content) were dissolved in water in a test tube at 60 °C and agitated to form a uniform suspension. The solution was laid for 48 h at ambient temperature, and then the suspension state was carefully observed.

2.4.7. Tensile tests

The stress–strain properties were measured according to ASTM D 412-80 specification using dumb-bell test pieces by an Instron 5567 Universal Testing Machine at a crosshead speed of 100 mm/min. At least five measurements for each sample were made in order to eliminate experimental error. All the samples were vacuum oven dried at 60 °C to reach a constant weight before testing.

2.4.8. Dynamic mechanical analysis

Dynamic mechanical analysis (DMA) was performed in tensile mode on a DMAQ800 analyzer (USA). Temperature scans at 1 Hz frequency were carried out at a heating rate of 5 °C/min from −30 to 210 °C. Samples of PVA/MCC composites were from the injection molding and were dried in vacuum oven at 60 °C for 24 h before testing.

3. Results and discussion

3.1. FTIR and FT-Raman analysis

Fig. 1(a) shows the FTIR spectra of WCFs and MCC. The absorption peak at 3416 cm^{-1} which ascribed to the stretching vibration of —OH groups of WCFs shifted toward lower wavelength after acid treatment, suggesting that the acid hydrolysis weakened the hydrogen bonding of cellulose (Ruan, Huang, & Zhang, 2005). The generation of free hydroxyl groups would benefit the formation of new hydrogen bonds with PVA. During the plasticization by formamide and water, the intra- and inter-molecular hydrogen bonds of PVA were broken. Consequently, the resulting free hydroxyl groups between formamide molecules and PVA molecules are expected to establish new hydrogen bonds during the melt-processing treatment. This claim is supported by FTIR spectra of neat PVA and PVA/MCC-0 composite as shown in Fig. 1(b). In this figure, the peaks at the wave numbers of 3416 cm^{-1} (the stretching vibration peak of its side hydroxyl groups), 2923 cm^{-1} (the —CH_2 group stretching

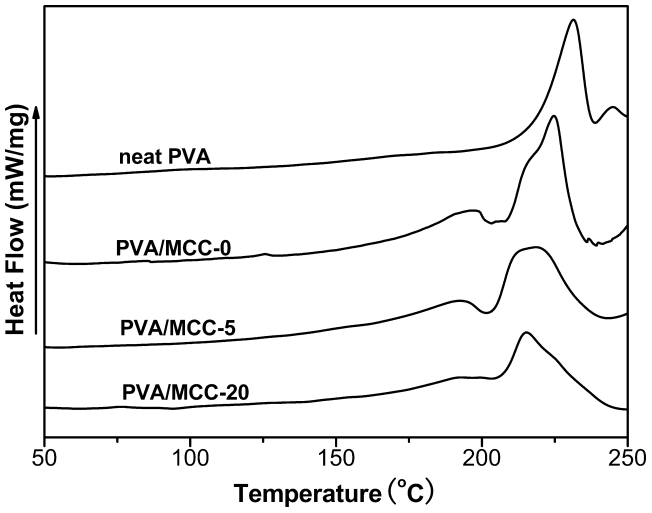

Fig. 2. DSC curves of neat PVA and PVA/MCC composites.

Table 1
Data from thermal analysis and crystallite size of neat PVA and PVA/MCC composites.[a]

Samples	T_m (°C)	T_{on} (°C)	T_p (°C)	$T_{on} - T_m$ (°C)	ΔH_m (J/g)	X_c (%)	Crystallite size (nm)
Neat PVA	230	228	260	–	81.9	50.9	9.51
PVA/MCC-0	225	246	264	21	77.2	47.9	9.22
PVA/MCC-5	219	254	274	35	68.7	44.9	8.74
PVA/MCC-20	215	269	291	54	45.0	35.0	8.76

[a] The *n* in PVA/MCC-*n* stands for MCC content relative to PVA, that is 0, 5%, 10%, 15%, 20% in weight, respectively.

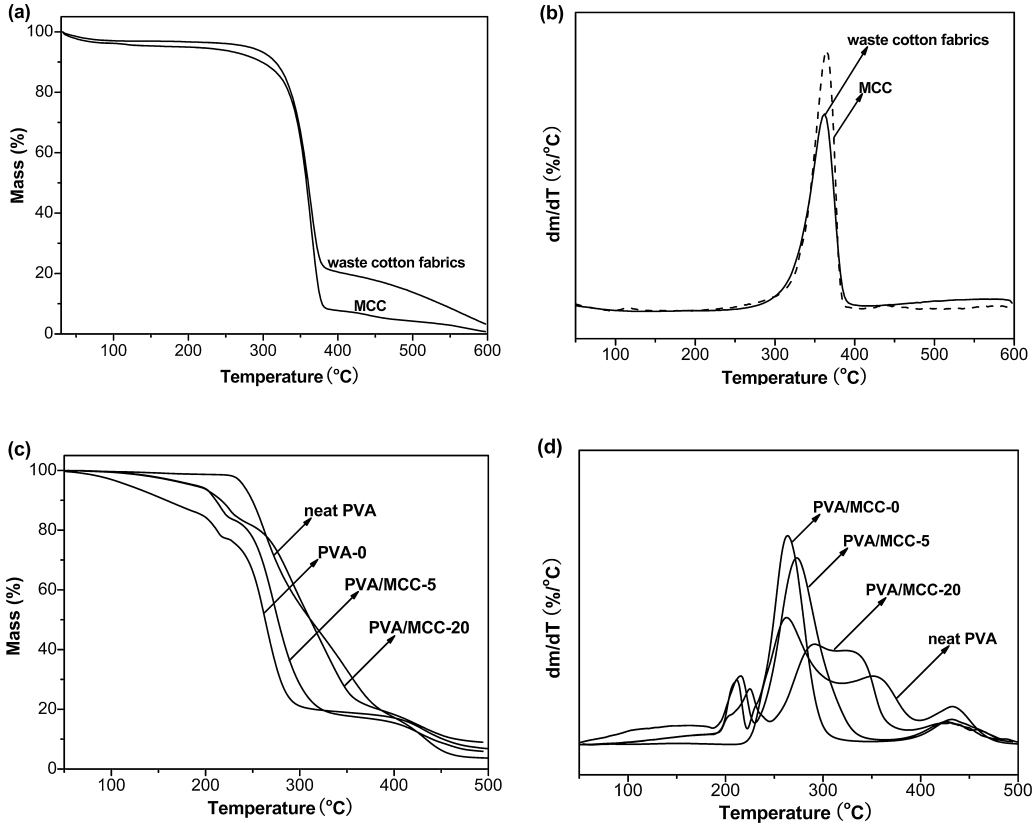

Fig. 3. TG curves of: (a) WCFs and MCC and (b) neat PVA and PVA/MCC composites. DTG curves of: (c) WCFs and MCC and (d) neat PVA and PVA/MCC composites.

vibration), 1145 cm^{-1} (crystalline domains of PVA) and 1096 cm^{-1} (the C—O group) are characteristic peaks of neat PVA (Chhatri et al., 2011; Lee et al., 2009). The absorption peak at 3416 cm^{-1} (the stretching vibration of —OH groups) of neat PVA blue shifts (19 cm^{-1}) after the addition of formamide and water which indicates that the hydrogen bond could be formed between —OH groups of PVA and the functional groups like $—NH_2$ and C=O of formamide. It can be also seen that the absorption peak at 1145 cm^{-1} slightly shifts toward the lower frequency after plasticization processing, suggesting the change of crystalline domains in PVA. The result is in accordance with the analysis of XRD as will be shown later.

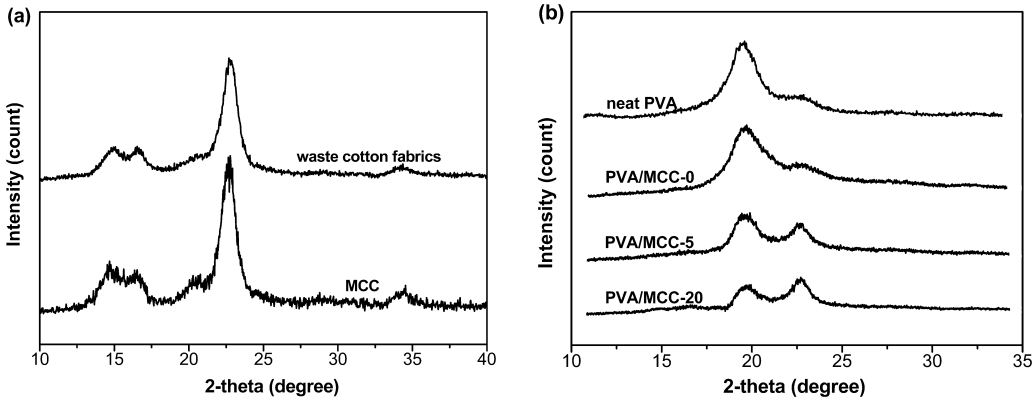

Fig. 4. XRD patterns of: (a) WCFs and MCC and (b) neat PVA and PVA/MCC composites.

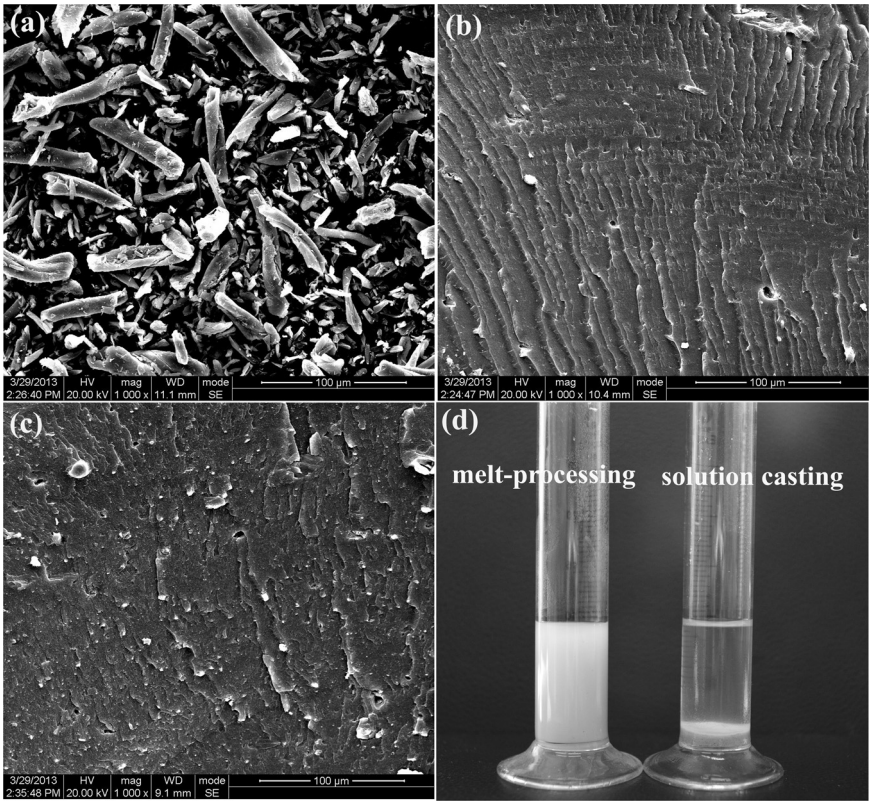

Fig. 5. Scanning electron micrographs of: (a) MCC, (b) PVA/MCC-5, (c) PVA/MCC-20 and (d) Molau test results of the samples in water.

The FT-Raman spectra of neat PVA and PVA/MCC composites are given in Fig. 1(c). In this figure, the peaks at the wave numbers of 2908, 1444, 1363, 1147, 1094, 917 and 856 cm^{-1} are attributed to neat PVA (Chhatri et al., 2011; Lin et al., 2003). It can be seen that the band intensity at 2908 cm^{-1} of PVA becomes weaker after the addition of plasticizer, and the band of PVA/MCC-20 becomes much narrower and weaker compared with PVA/MCC-0, which indicates that PVA chain structure changed with the addition of formamide and MCC. The peaks at 1094 and 1147 cm^{-1} correspond to the infrared "crystallinity sensitive" band and dependent upon the crystallinity of PVA (Iwamoto, Miya, & Mima, 1979). These bands of PVA become weaker with the addition of MCC, which suggests the crystallization of PVA is suppressed by MCC. This result might be ascribed to the inter-molecular complexes formed through hydrogen bonding between MCC and PVA.

3.2. Thermal property analysis

The key point to realize melt-processing of PVA is to decrease its T_m and increase its T_{on}, thus expanding its melt-processing window ($T_{on} - T_m$). DSC curves obtained from neat PVA and PVA/MCC composites are shown in Fig. 2. The melting peak shows an obvious shift to lower temperature with the increase of MCC content. The DSC data of neat PVA and PVA/MCC composites are summarized in Table 1. The T_m of PVA decreases from 230 to 215 °C with the incorporation of 20 wt% MCC. Simultaneously, it could be found that when formamide and water was added to PVA, ΔH_c and X_c decreased remarkably as a result, suggesting that plasticizer could destroy the crystalline structure of PVA. The results indicated that formamide and water reduced the interaction of PVA chains and facilitated their chain movement. When MCC was added to PVA, such an effect was even greater. This phenomenon can be ascribed to the fact that MCC have a strong interaction with PVA as well, and they will further destroy regular arrangement of molecular chains. Higher filler dispersion and interfacial adhesion is thought to hinder polymer chains regular rearrangements to some extent and hence inhibited crystallization of PVA.

Fig. 3 shows the TG and DTG curves of WCFs, MCC, neat PVA and PVA/MCC composites. As shown in Fig. 3(a) and (b), MCC has similar thermal stability compared with WCFs. There is a single degradation step for WCFs and MCC, which starts from about 326 °C and shows maximum decomposition at around 355 °C. This result indicates that acid hydrolysis do not reduce the thermal stability of cellulose. Fig. 3(c) shows that there are two major weight losses for neat PVA and PVA/MCC composites in the range of 200–500 °C, which could be attributed to the structural decomposition of PVA (Lu, Wang, & Drzal, 2008). All PVA/MCC samples show a small peak at about 205 °C in derive curves (Fig. 4(c)), which is due to the evaporation of formamide in the composites. As indicated in Fig. 3(c) and (d), the onset decomposition temperature and the major degradation peak temperature of PVA/MCC composites notably shift toward higher temperature with the increase of MCC content, which demonstrating that MCC significantly improved the thermal stability of the composites. The enhancement of thermal stability of PVA with the incorporation of MCC could be explained by the higher stability of the MCC and particularly by the excellent compatibility between MCC and PVA matrix.

It is obvious that the T_m of the PVA/MCC composites moves to lower temperature and the T_{on} moves to higher temperature with the increase of MCC content as shown in Table 1. As a result, the melt-processing window was remarkably expanded. A melt-processing window of 54 °C is achieved when the content of MCC reaches 20 wt%.

3.3. XRD analysis

X-ray diffraction (XRD) is a powerful instrument for characterization of polymer crystalline structure. Fig. 4 shows the XRD

patterns of WCFs and MCC (Fig. 4(a)), neat PVA and PVA/MCC composites (Fig. 4(b)). As shown in Fig. 4(a), the diffractograms of WCFs and MCC exhibit main crystal planes of the crystalline cellulose I structure with the main characteristic peaks localized at 14.9°, 16.8°, 22.8° and 34.5°, which are assigned to the diffraction planes of 101, 101, 002, and 040, respectively (El-Sakhawy & Hassan, 2007; Gindl & Keckes, 2005). The results indicated that the crystalline structure of WCFs was essentially maintained in the MCC particles. On the other hand, the crystallinity index of MCC was calculated to be 87.1% through intensity measurements at 22° and 19° (amorphous background) according to the report by Levis and Deasy (2001). As shown in Fig. 4(b), neat PVA exhibits a significant crystalline peak at about 19.4° that assigned to the diffraction planes of 200, which was due to the strong inter- and intramolecular hydrogen bonding (Lu et al., 2008; Zhang et al., 2007). Obviously, with the addition of MCC into PVA matrix, the diffractograms of the composites display the characteristic peaks of the two components. The intensity of the diffraction peaks resulted from MCC increases with the increase of MCC content. Based on intermolecular complexation, formamide and MCC has a potential to form new hydrogen bonding with PVA by replacing the intra- and intermolecular hydrogen bonding of PVA. In this way, the crystallization of PVA was inhibited. Fig. 4(b) shows the crystalline peaks of neat PVA are significantly weakened after the plasticization with formamide and water. Meanwhile, the intensity of the diffraction peak of the PVA/MCC composites at about 19.4° became lower and narrower with the increase of MCC content. Furthermore, the crystallite size of PVA decreases from 9.51 to 8.76 nm with the incorporation of 20 wt% MCC (Table 1). This is probably because the presence of MCC can induce a restricted mobility of PVA chains by forming hydrogen bonds in the interface, which is corresponded with the DSC result. This effect could be used to enhance the thermal and mechanical properties of the composites.

3.4. Morphological analysis

Under a drastic condition of acid hydrolysis, cellulose chains cause bond cleavage, i.e., hydrolytic cleavage of glycosidic bonds between two anhydroglucose units, producing short-chain cellulose. The amorphous component was reduced to acid-soluble end products, leaving behind the crystalline regions. Acid hydrolysis followed by mechanical stirring results in disintegration of cellulose into small irregular MCC particles (Das et al., 2009). Fig. 5(a) shows the SEM image of MCC. As seen from the figure that shortening of fibers occurred and rod-like MCC particles were formed. The particle size of the prepared MCC is irregular with broad particle size distribution from several to tens of microns.

The degree of dispersion and the bonding ability between matrix and reinforcing phase is one of the most critical factors in determining the properties of any composite materials (Mathew et al., 2005). Fig. 5(b) and (c) shows the SEM images of PVA/MCC composites with 5 wt% (Fig. 5(b)) and 20 wt% (Fig. 5(c)) MCC, respectively. It can be seen that there are well-dispersed bright dots and short rods on the fractured section of composites, which are consistent with the ends of MCC in the polymer matrix. No large agglomerates of the fillers and good adhesion between the matrix and fillers are observed, which should play an important role in improving the mechanical performance and thermal properties of the resulting materials.

3.5. Molau test

In the Molau test (Tian, Chen, & Guo, 2005), polymer-based composites were dissolved in solvent and then the dispersion state of the solution is observed. If the interfacial interaction between two components of the composites was not formed, the solution would separate into two parts; otherwise, the two components of solution would not be separated even after a long time, and a persistent turbidity comes into view. The Molau test results are shown in Fig. 5(d). It can be seen that MCC in melt-processed PVA/MCC composites is well distributed in solution after 48 h and the sediment is not obviously. However, the solution of PVA/MCC film prepared by solution casting was separated into two parts quickly (20 min) – a clear solution containing PVA on the top of test tube and the deposition of MCC particles at the bottom. The results indicate that MCC could establish strong interfacial interaction with PVA through hydrogen bonding after melt-processing.

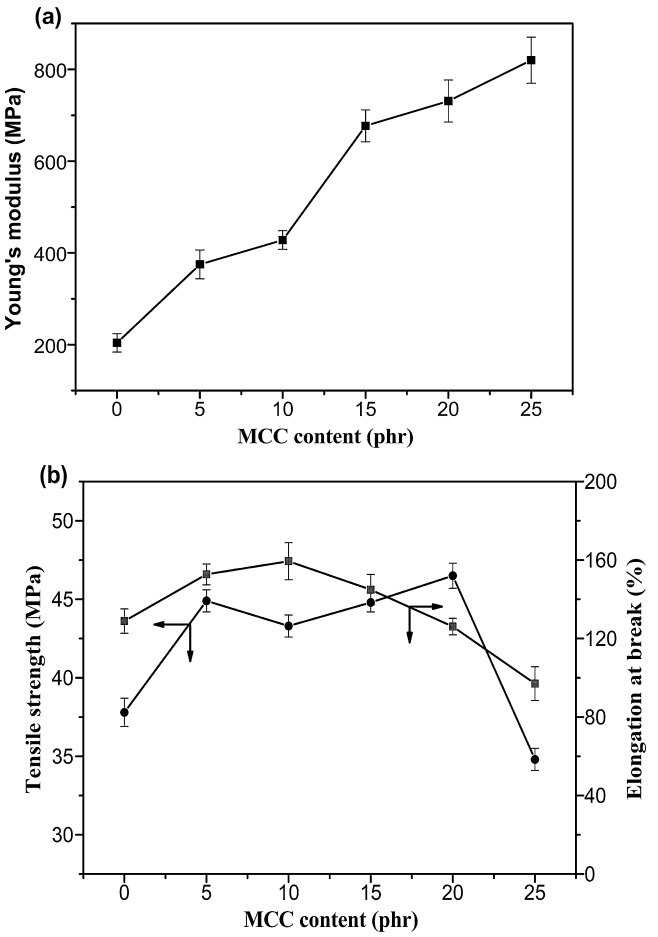

Fig. 6. (a) Young's modulus and (b) tensile strength and elongation at break as the function of MCC content.

3.6. Mechanical properties

The compound of MCC is also expected to improve tensile properties of the PVA/MCC composites. Fig. 6 shows the Young's modulus (Fig. 6(a)) and tensile strength, elongation at break (Fig. 6(b)) of PVA/MCC composites. The Young's modulus of PVA/MCC composites increases with increasing MCC content. Compared with the modulus of PVA/MCC-0 (204.8 MPa), that of PVA/MCC-20 (731.2 MPa) significantly increased by 257.0%. A similar increase of Young's modulus was reported by Zimmermann, Pöhler, and Geiger (2004), for cellulose fibrils isolated from sulphite pulp reinforced PVA composites. This outstanding property may be attributed to the formation of a networked structure above percolation threshold (Samir, Alloin, & Dufresne, 2005) which was produced by cellulose fibers interactions through hydrogen bonding. In general, the Young's modulus of polymers can be increased by the reinforcement of cellulose fibers, while the tensile strength

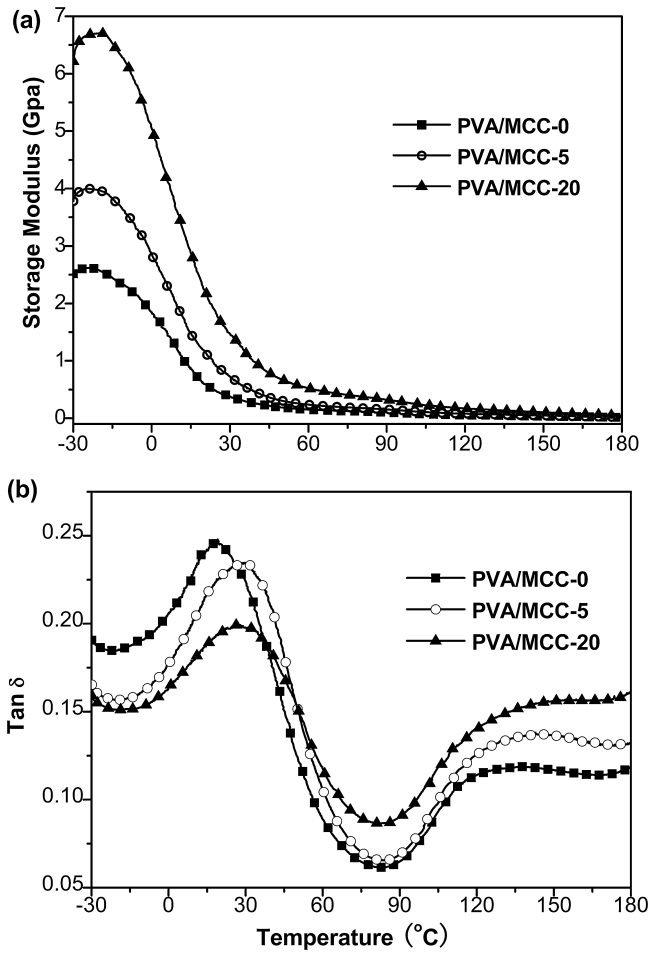

Fig. 7. (a) Storage modulus and (b) tan δ versus temperature for PVA/MCC composites.

does not improve or sometimes decreases due to flocculation of cellulose fibers (Ibrahim, El-Zawawy, & Nassar, 2010). For example, Mathew et al. (2005) reported that the incorporation of MCC has a negative effect on the tensile strength of poly(lactic acid), which was decreased from its original 49.6 to 38.2 MPa with the addition of 10 wt% MCC. However, it is apparent that the incorporation of MCC into the PVA led to an improvement in tensile strength (Fig. 6(b)) and Young's modulus simultaneously in this study. The tensile strength of PVA/MCC composites increased from 37.8 to 46.5 MPa by 23.0%. These results further confirm the presence of strong interfacial interaction and good dispersion between MCC and PVA. The tensile strength decreased apparently when the content of MCC is above 25 phr, which may be attributed to the aggregation of MCC at higher filler content. On the other hand, there is no obvious decrease in the elongation at break of the PVA/MCC composites with increasing MCC content, which is favorable for the performance of the composites.

3.7. Dynamic mechanical analysis

Fig. 7 shows the storage modulus and tan δ versus temperature for PVA/MCC composites. In Fig. 7(a), it can be seen that the storage modulus of all the samples decreases with increasing temperature. The PVA/MCC composites show an increasing trend of storage modulus as compared with PVA/MCC-0 over the entire temperature span, suggesting improved thermal–mechanical properties of the composites. When the MCC content reaches 20 wt%, the storage modulus exhibits a remarkable increment. This result is in accordance with tensile testing due to the strong interfacial interactions through hydrogen bonding between MCC with large specific surface and PVA matrix. The improvement in storage modulus was most significant before 60 °C, where the molecular relaxation occurs for PVA.

By incorporating MCC into PVA matrix, the glass transition temperature (T_g) of PVA shifts to higher temperature from 17.6 to 30.3 °C. The increase in T_g due to the incorporation of MCC might be attributed to the occurrence of intermolecular interactions occurred between MCC and PVA matrix, which reduces the flexibility of molecular chains of PVA (Tsagaropoulos & Eisenberg, 1995). This behavior is consistent with the results of previous studies dealing with the preparation of MCC-reinforced polymer composites (Mathew et al., 2005; Spoljaric et al., 2009). Furthermore, a slight decrease in the tan δ peak at T_g is observed with increasing MCC content (Fig. 7(b)). Apparently, a smaller proportion of the PVA matrix participated in the glass transition when MCC were present. This indicates favorable matrix–fiber interaction and possibly the formation of an interphase matrix layer, either immobilized or of reduced molecular mobility (Wu, Henriksson, Liu, & Berglund, 2007).

4. Conclusion

Recycling WCFs into the value-added products is an attractive option for environmental and economic benefits. We have demonstrated a viable and efficient approach to prepare ecocomposites based on plasticized PVA and MCC extracted from WCFs through melt-processing. The waste-derived MCC was used as reinforcement to enhance melt-processability of PVA, using formamide and water as plasticizer. It was shown that formamide and MCC could form inter-molecular complexes with PVA through hydrogen bonding and confine the crystallization of PVA. The melt-processing window of PVA/MCC composites was expanded up to 54 °C with the incorporation of 20 wt% MCC, and the mechanical properties of the resulting PVA/MCC composites were significantly improved. This work aims at demonstrating the value-added utilization of waste cotton fabrics and the feasibility of making WCFs-based high performance ecocomposites on industrial-scale production.

Acknowledgments

The authors would like to thank the National Science Foundation of China (51203105) and National High Technology Research and Development Program (863 Program, SS2012AA062613) for financial support.

References

Cheng, Q., Wang, S., & Rials, T. G. (2009). Poly(vinyl alcohol) nanocomposites reinforced with cellulose fibrils isolated by high intensity ultrasonication. *Composites: Part A*, *40*, 218-214.

Chhatri, A., Bajpai, J., Bajpai, A. K., Sandhu, S. S., Jain, N., & Biswas, J. (2011). Cryogenic fabrication of savlon loaded macroporous blends of alginate and polyvinyl alcohol (PVA). Swelling, deswelling and antibacterial behaviors. *Carbohydrate Polymers*, *83*, 876–882.

Chuayjuljit, S., Su-Uthai, S., Tunwattanaseree, C., & Charuchinda, S. (2009). Preparation of microcrystalline cellulose from waste-cotton fabric for biodegradability enhancement of natural rubber sheets. *Journal of Reinforced Plastics and Composites*, *28*, 1245–1254.

Chuayjuljit, S., Su-Uthai, S., & Charuchinda, S. (2012). Poly(vinyl chloride) film filled with microcrystalline cellulose prepared from cotton fabric waste: Properties and biodegradability study. *Waste Management & Research*, *28*, 109–117.

Das, K., Ray, D., Bandyopadhyay, N. R., Ghosh, T., Mohanty, A. K., & Misra, M. (2009). A study of the mechanical, thermal and morphological properties of microcrystalline cellulose particles prepared from cotton slivers using different acid concentrations. *Cellulose*, *16*, 783–793.

El-Sakhawy, M., & Hassan, M. L. (2007). Physical and mechanical properties of microcrystalline cellulose prepared from agricultural residues. *Carbohydrate Polymers*, *67*, 1–10.

Engelhardt, A. W. (2010). *A world survey on textile and nonwovens industry*. *The Fiber Year 2009/10* (10) Switzerland: Oerlikon (view all references).

Gindl, W., & Keckes, J. (2005). All cellulose nanocomposite. *Polymer*, *46*, 10221–10225.
Haafiz, M. K. M., Eichhorn, S. J., Hassan, A., & Jawaid, M. (2013). Isolation and characterization of microcrystalline cellulose from oil palm biomass residue. *Carbohydrate Polymers*, *93*, 628–634.
Ibrahim, M. M., El-Zawawy, W. K., & Nassar, M. A. (2010). Synthesis and characterization of polyvinyl alcohol/nanospherical cellulose particle films. *Carbohydrate Polymers*, *79*, 694–699.
Isci, A., & Demirer, G. N. (2007). Biogas production potential from cotton wastes. *Renew Energy*, *32*, 750–757.
Iwamoto, R., Miya, M., & Mima, S. (1979). Determination of crystallinity of swollen poly (vinyl alcohol) by laser Raman spectroscopy. *Journal of Polymer Science Polymer Physics*, *17*, 1507–1515.
Jeihanipour, A., & Taherzadeh, M. J. (2009). Ethanol production from cotton-based waste textiles. *Bioresource Technology*, *100*, 1007–1010.
Jia, Y., Gong, J., Gu, X., Kim, H., Dong, J., & Shen, X. (2007). Fabrication and characterization of poly (vinyl alcohol)/chitosan blend nanofibers produced by electrospinning method. *Carbohydrate Polymers*, *67*, 403–409.
Kadokawa, J., Takegawa, A., Mine, S., & Prasad, K. (2011). Preparation of chitin nanowhiskers using an ionic liquid and their composite materials with poly(vinyl alcohol). *Carbohydrate Polymers*, *84*, 1408–1412.
Lee, H. W., Karim, M. R., Park, J. H., Ghim, H. D., Choi, J. H., Kim, K., et al. (2009). Poly(vinyl alcohol)/chitosan oligosaccharide blend submicrometer fibers prepared from aqueous solutions by the electrospinning method. *Journal of Applied Polymer Science*, *1*, 132–140.
Levis, S. R., & Deasy, P. B. (2001). Production and evaluation of size reduced grades of microcrystalline cellulose. *International Journal of Pharmaceutics*, *213*, 13–24.
Lin, Y., Zhou, B., Fernando, K. A. S., Liu, P., Allard, L. F., & Sun, Y. (2003). Polymeric carbon composites from carbon nanotubes functionalized with matrix polymer. *Macromolecules*, *36*, 7199–7204.
Lu, J., Wang, T., & Drzal, L. T. (2008). Preparation and properties of microfibrillated cellulose polyvinyl alcohol composite materials. *Composites: Part A*, *39*, 738–746.
Mathew, A. P., Oksman, K., & Sain, M. (2005). Mechanical properties of biodegradable composites from poly lactic acid (PLA) and microcrystalline cellulose (MCC). *Journal of Applied Polymer Science*, *97*, 2014–2025.
Miranda, R., Sosa-Blanco, C., Bustos-Martinez, D., & Vasile, C. (2007). Pyrolysis of textile wastes: I. Kinetics and yields. *Journal of Analytical and Applied Pyrolysis*, *80*, 489–495.
Molau, G. E., & Wittbrodt, W. M. (1968). Colloidal properties of styrene-butadiene block copolymers. *Macromolecules*, *1*, 260–264.
Nishio, Y., & Manley, R. S. J. (1998). Cellulose-poly (vinyl alcohol) blends prepared from solutions in N,N-dimethylacetamide-lithium chloride. *Macromolecules*, *21*, 1270–1277.
Ratanakamnuan, U., Atong, D., & Aht-Ong, D. (2012). Cellulose esters from waste cotton fabric via conventional and microwave heating. *Carbohydrate Polymers*, *87*, 84–94.
Ruan, D., Huang, Q., & Zhang, L. (2005). Structure and properties of CdS/regenerated cellulose nanocomposites. *Macromolecular Materials and Engineering*, *290*, 1017–1024.
Samir, M. A. S. A., Alloin, F., & Dufresne, A. (2005). Review of recent research into cellulosic whiskers, their properties and their application in nanocomposite field. *Biomacromolecules*, *6*, 612–626.
Saowaroj, C., Su-Uthai, S., & Charuchinda, S. (2010). Poly(vinyl chloride) film filled with microcrystalline cellulose prepared from cotton fabric waste: Properties and biodegradability study. *Waste Management & Research*, *28*, 109–117.
Shen, F., Xiao, W., Lin, L., Yang, G., Zhang, Y., & Deng, S. (2013). Enzymatic saccharification coupling with polyester recovery from cotton-based waste textiles by phosphoric acid pretreatment. *Bioresource Technology*, *130*, 248–255.
Spoljaric, S., Genovese, A., & Shanks, R. A. (2009). Polypropylene-microcrystalline cellulose composites with enhanced compatibility and properties. *Composites: Part A*, *40*, 791–799.
Tian, M., Chen, G., & Guo, S. (2005). Effect of high-energy vibromilling on interfacial interaction and mechanical properties of PVC/nano-$CaCO_3$ composites. *Macromolecular Materials and Engineering*, *290*, 927–932.
Tsagaropoulos, G., & Eisenberg, A. (1995). Dynamic mechanical study of the factors affecting the two glass transition behavior of filled polymers. Similarities and differences with random ionomers. *Macromolecules*, *28*, 6067–6077.
Uddin, A. J., Fujie, M., Sembo, S., & Gotoh, Y. (2012). Outstanding reinforcing effect of highly oriented chitin whiskers in PVA nanocomposites. *Carbohydrate Polymers*, *87*, 799–805.
Wu, Q., Henriksson, M., Liu, X., & Berglund, L. A. (2007). A high strength nanocomposite based on microcrystalline cellulose and polyurethane. *Biomacromolecules*, *8*, 3687–3692.
Xiong, R., Lu, C., Zhang, W., Zhou, Z., & Zhang, X. (2013). Facile synthesis of tunable silver nanostructures for antibacterial application using cellulose nanocrystals. *Carbohydrate Polymers*, *95*, 214–219.
Xiong, R., Zhang, X., Tian, D., Zhou, Z., & Lu, C. (2012). Comparing microcrystalline with spherical nanocrystalline cellulose from waste cotton fabrics. *Cellulose*, *19*, 1189–1198.
Zhang, Y., Huang, X., Duan, B., Wu, L., Li, S., & Yuan, X. (2007). Preparation of electrospun chitosan/poly(vinyl alcohol) membranes. *Colloid and Polymer Science*, *285*, 855–863.
Zhen, W., Lu, C., Li, C., & Liang, M. (2012). Structure and properties of thermoplastic saponite/poly(vinyl alcohol) nanocomposites. *Applied Clay Science*, *57*, 64–70.
Zia, K. M., Zuber, M., Rizwan, A., Jamil, T., Tabasum, S., & Shahid, M. (2012). Modification of cellulosic fabric using polyvinyl alcohol—Part-I: Physicochemical properties. *Carbohydrate Polymers*, *87*, 2063–2067.
Zimmermann, T., Pöhler, E., & Geiger, T. (2004). Cellulose fibrils for polymer reinforcement. *Advanced Engineering Materials*, *6*, 754–761.
Zuber, M., Zia, K. M., Bhatti, I. A., Jamil, T., Fazal-ur-Rehman, & Rizwan, A. (2012). Modification of cellulosic fabric using polyvinyl alcohol—Part-II: Colorfastness properties. *Carbohydrate Polymers*, *87*, 2439–2446.